JTCM Journal of Traditional Chinese Medicine

Online Submissions: http://www.journaltcm.com
ISSN 0255-2922
info@journaltcm.com

Original Article

Efficacy of active ingredients in Qingdai (*Indigo Naturalis*) on ulcerative colitis: a network pharmacology-based evaluation

LI Yue, WEN Shuting, ZHAO Runyuan, FAN Dongmei, ZHAO Dike, LIU Fengbin, MI Hong

LI Yue, Department of orthopedics, the First Affiliated Hospital of Guangzhou University of Chinese Medicine, Guangzhou 510405, China
WEN Shuting, ZHAO Runyuan, the First School of Clinical Medicine, Guangzhou University of Chinese Medicine, Guangzhou 510405, China
ZHAO Dike, Basic Medical College, Henan University of Chinese Medicine, Zhengzhou 450046, China
FAN Dongmei, LIU Fengbin, Department of Gastroenterology, the First Affiliated Hospital of Guangzhou University of Chinese Medicine, Guangzhou 510405, China
Supported by Natural Science Foundation of Guangdong Province: Mechanism of Chang-An Decotion in Neuropeptide Spexin related GSK-3 β Regulating Intestinal Nerve Immune Network in Ulcerative Colitis (No. 2018A030310614), National Natural Science Foundation of China: Mchanism of Chang-An Decotion in Intestinal Mucosal Immunity of Ulcerative Colitis on Exocrine Mediated Rab27 (No. 81903963), Department of Education of Guangdong Province Project: Mchanism of Chang-An decotion of Ulcerative Colitis on Exocrine Mediated GSK-3 β Regulating Th17/Treg in Ulcerative Colitis (No. (2017KQNCX045)
Correspondence to: Dr. MI Hong, Department of Gastroenterology, the First Affiliated Hospital of Guangzhou University of Chinese Medicine, Guangzhou 510405, China. mihong10000@163.com
Telephone: +86-15920583726
DOI: 10.19852/j.cnki.jtcm.2023.01.011
Received: November 29, 2021
Accepted: February 11, 2022
Available online: January 10, 2023

Abstract

OBJECTIVE: To elucidate the protective effect of Qingdai (*Indigo Naturalis*, QD) on ulcerative colitis (UC) by means of *in silico* and *in vivo* approaches.

METHODS: A systems pharmacology analysis was performed to predict the active components of QD whereas the putative biological targets of QD against UC were obtained through target fishing, network cons-truction and enrichment analyses. Meanwhile, we examined the ameliorative effect of QD in a mouse model of dextran sulfate sodium (DSS)-induced colitis. During the 10-day experiment, the control and diseased mice were given with oral gavages of QD (1.3 g raw herbs • kg^{-1} • d^{-1}) or 5-aminosalicylic acid (5-ASA, 100 mg • kg^{-1} • d^{-1}) every day. The underlying pharma-cological mechanisms of QD in UC were determined using polymerase chain reaction tests, histological staining, enzyme-linked immunoassays, and Western blotting analysis.

RESULTS: Searching from various network pharmacology databases, 29 compounds were identified in QD. According to the screening criteria suggested by TCMSP (i.e. OB ≥ 30% and DL ≥ 0.18), nine of them were considered the active ingredients that contribute to the ameliorative effects of QD on different mouse models of colitis. Most importantly, the protective effect of QD on DSS-induced colitis was significantly associated with modulations of the expression levels of glycogen synthase kinase 3-β (Gsk3-β) and forkhead box p3 (Foxp3), which are widely considered as important regulators of excessive inflammatory responses.

CONCLUSIONS: The results of this study provide solid scientific evidence for the use of QD or its core active components in the clinical management of UC.

Keywords: Qingdai (*Indigo Naturalis*); colitis, ulcerative; glycogen synthase kinase 3 beta; signaling transduction; forkhead transcription factors; network pharmacology

1. INTRODUCTION

Ulcerative colitis (UC) is a nonspecific inflammatory disease of the gastrointestinal tract;[1] however, the pathogenesis of UC has yet to be fully elucidated, and current medical treatment options aim to minimize the recurrence of flare-ups.[2] The first-line therapeutics for UC include 5-aminosalicylic acid (5-ASA), gluco-corticoids, immunosuppressants, and biological agents.[2] However, the effectiveness of these current therapeutics is barely satisfactory, as the recurrence rate of UC remains high in many patients. As a result, UC patients tend to seek alternative treatment options to alleviate their symptoms; Traditional Chinese Medicine (TCM) has become one of the most common forms of complementary and alternative medicine (CAM) in the clinical management of UC.[3] In fact, various TCM formulations have been widely used in the prevention and treatment of UC in China for a long time.[4] In particular, Qingdai (*Indigo Naturalis*, QD) has been shown to be beneficial as a UC treatment in clinical trials.[5]

In general, QD is extracted from the leaves or stems of medicinal plants of the Acanthaceae, Polygonaceae and Brassicaceae (or Cruciferae) families, such as Isatis indigotica, as dry powder, agglomerates or granules.[6] According to TCM principles, QD is responsible for detoxification and the clearance of "heat" while possessing some blood-cooling and shock-reducing properties. In this study, we aimed to elucidate the protective mechanisms of QD against UC using a mouse model of dextran sulfate sodium (DSS)-induced colitis. In addition to the *in vivo* experiment, network pharmacology databases were used to predict and explain the active compounds of QD, as well as their biological targets related to the amelioration of UC. Indeed, the holistic and systematic nature of network pharmacology correlates well with syndrome-symptom pattern based TCM treatment approaches.[7] Based on the comprehensive network pharmacology analyses, this study aimed to investigate solid scientific evidence for the use of QD or its core active components in the clinical management of UC.

2. MATERIALS AND METHODS

2.1. Systems pharmacology screening of active compounds of QD

All the active compounds of QD were obtained from the Traditional Chinese Medicine System Pharmacology Analysis Platform (TCMSP; http://lsp.nwu.edu.cn/tcmsp.php).[8] By means of *in silico* integrative pharmacokinetic evaluation suggested by TCMSP, candidate compounds with values of oral bioavailability (OB) ≥ 30% and drug-likeness (DL) ≥ 0.18 were selected for our further analyses.

2.2. Construction of compound-target network

For an overall exploration of the plausible pharmacological mechanisms of QD, the putative targets of the selected active compounds were searched *via* TCMSP, BATMAN-TCM (http://bionet.ncpsb.org.cn/batman-tcm/),[9] TCMID (http://bidd.group/TCMID/),[10] Swiss Target Prediction (http://www.swisstargetprediction.ch/)[11] and PharmMapper (http://lilab-ecust.cn/pharmmapper/index.html).[12] The QD-target network was constructed using the Cytoscape 3.7.1 visualization software (http://www.cytoscape.org/).[13]

2.3. Identification of disease-related targets

The known UC-related targets were attained from various databases, including the Online Mendelian Inheritance in Man database (OMIM; http://www.omim.org/),[14] Therapeutic Target Database (TTD; http://db.idrblab.net/ttd/),[15] Pharmacogenomics Knowledgebase (PHARMGKB; https://www.pharmgkb.org/)[16] and Genetic Association Database (GAD; http://geneticassociationdb.nih.gov/),[15] as well as text mining tools, such as DiGSeE (http://210.107.182.61/geneSearch),[17] Pathway Assembly from Literature Mining-and Information Search Tool (PALM-IST; http://www.hpppi.iicb.res.in/ctm/index.html),[18] PolySearch2 (http://polysearch.cs.ualberta.ca)[19] and COREMINE (http://www.coremine.com/medical).[20] At the pathway level, the UC-related target proteins were obtained from the GEO DataSets with the species limited to *Homo sapiens*, expression profiling limited to arrays with sample size ≥ 100 and the log fold change (logFC) value at ≥ 0.585 (i.e. the absolute FC value at ≥ 1.5). Further, the differential gene targets of the array analyses were compared using the GEO2R software (https://www.ncbi. nlm.nih.gov/geo/geo2r/) whereas the UC-related datasets were presented using the Venn diagram (http://bioinfogp.cnb.csic.es/tools/venny/index. html).

2.4. Network construction and analysis of QD on UC

In order to illustrate the role of target proteins at the system level, the relevant targets acquired from the Venn diagram intersection were imported into STRING[21] (http://string-db.org) and complemented with a cut-off confidence score set at > 0.7 to obtain more credible data. The Protein-protein interaction (PPI) networks for active compounds of QD and UC-related targets were then established, and visualized using the Cytoscape 3.7.1 software. An intersection was performed to identify the putative targets of QD against UC. For core target enrichment, Gene ontology (GO) and Kyoto Encyclopedia of Genes and Genomes (KEGG) enrichment analyses were subsequently performed using the clusterProfiler, AnnotationHub, AnnotationDbi, GOplot and ggplot2 libraries. A false discovery rate (FDR) < 0.05 is considered to be an important functional category and regulatory pathway involved in the treatment of UC.

2.5. Experimental animals

C57/BL6 mice (Specific pathogen free grade) aged 6-7 weeks old were purchased from the Guangdong Medical Laboratory Animal Center (Guangzhou, China, No. 44007200051619). The handling of mice and all experimental procedures were performed in accordance with the guidelines of the SPF Animal Experiment Center of the First Affiliated Hospital of Guangzhou University of Chinese Medicine (Ethics No. SYXK 2013-0092).

2.6. Induction of colitis and drug treatment

Thirty-two mice were randomly assigned into 4 groups (n = 8/group) according to the experimental design outlined in Figure S1. Experimental colitis was induced by giving the mice drinking water *ad libitum* containing 2.5% DSS (MW: 36 000-50 000 Da) for 7 d followed by an additional consumption period of normal drinking water for 3 d. Group 1: saline treatment control (designated CON); Group 2: 2.5% DSS treatment (designated DSS); Group 3: 2.5% DSS treatment plus oral gavage (o.g.) of 5-ASA (designated 5-ASA + DSS); Group 4: 2.5% DSS treatment plus o.g. of QD

(designated QD + DSS). The mice in the CON group were fed with drinking water without DSS and saline (o.g.) whereas the mice in the DSS group were fed with water containing 2.5% DSS and saline (o.g.) throughout the whole experimental period. While fed with 2.5% DSS, the mice in groups 3 and 4 were respectively given with 5-ASA (o.g.; 100 $mg \cdot kg^{-1} \cdot d^{-1}$) and QD (o.g.; 1.3 g raw $herbs \cdot kg^{-1} \cdot d^{-1}$) from day 0 till the end of experiment for a total of 10 d. The dosage of QD was equivalent to the typical clinical dosage (i.e. 0.15 g raw $herbs \cdot kg^{-1} \cdot d^{-1}$) for humans. During the 10-day trial, body weight, stool consistency and result of fecal occult blood test were recorded daily.

2.7. Macroscopic evaluation of severity of colitis

The severity of colitis in mice was assessed based on the loss of body weight, the scoring of stool consistency and the presence of fecal occult blood as we previously reported. The score of body weight loss was determined as follows: 0: (< 1% change of body weight); 1: (1-5%); 2: (6-10%); 3: (11-15%); 4: (> 15%). The score of stool consistency was ranging from 0 (i.e. normal, no diarrhea) to 4 (i.e. rotten and watery stool). The presence of fecal occult blood was determined as follows: 0: negative; 2: moderate; 4: severe. The disease activity index (DAI) was calculated by combining the percentage of body weight loss, the score of stool consistency and the score of fecal occult blood test (Table S1).

2.8. Histological examination of colonic sections

After mice were sacrificed, distal colons were harvested. Samples were sectioned into 4 μm slices and subjected to standard hematoxylin and eosin (HE) staining for the evaluation of colonic architecture, loss of crypts, mucosal damage and lymphocyte infiltration. Images were examined and captured using the Nikon microscope (Nikon Corporation, Tokyo, Japan).

2.9. Western blotting analysis

The dissected colon segments were rinsed with phosphate buffer saline 2-3 times. Proteins were extracted from the colonic tissues using ice-cold radio-immunoprecipitation assay buffer containing protease inhibitor. Protein content in each colonic sample was quantified using the bicinchoninic acid protein assay kit from Beyotime Institute of Biotechnology (Shanghai, China). The chemiluminescent reactions were then detected and captured by ChemiDoc fromBio-Rad Laboratories (Hercules, CA, USA). Protein bands were analyzed and quantified using the ImageJ software (National Institutes of Health, City of Baltimore, MD, USA).

2.10. Real-time quantitative polymerase chain reaction (qRT-PCR)

Total RNA was extracted from colonic tissuesand transcribed into cDNA using the PrimeScript RT master mix from TaKaRa biotechnology (Tokyo, Japan) according to the manufacturer's instructions. The cDNA templates were then amplified with mouse-specific primers for Gsk3-β and Foxp3 using the TB Green™ Premix Ex Taq™ II from TaKaRa biotechnology (Tokyo, Japan). The target sequences were amplified with a hot start at 95 ℃ 3 min and 40 denaturation cycles at 95 ℃ for 15 s, annealing at 60 ℃ for 60 s and elongating at 72 ℃ for 40 s. The primers were designed using the online tool Primer-BLAST, and the sequences are listed in Table S2. Expression of gene of interest of each sample was normalized to the endogenous control β-actin, and semi-quantified using the comparative Ct method. Each experiment was performed in triplicate.

2.11. Biochemical assessment of pro-inflammatory mediators

Colonic tissues (10% w/v) were homogenized in ice-cold potassium phosphate buffer containing protease inhibitor followed by two cycles of sonication. The colonic levels of pro-inflammatory cytokines namely tumor necrosis factor-α (TNF-α), interleukin (IL)-1β and IL-17a were measured using enzyme-linked immunosorbent assays (ELISAs, AndyGene Co., Ltd., Shanghai, China) according to manufacturer's instructions.

2.12. Statistical analysis

The statistical differences were determined using SPSS 21.0 (IBM Corp., Armonk, NY, USA), and the results are all expressed as mean ± standard derivation ($\bar{x} \pm s$). Kruskal-Wallis one-way analysis of variance was used for comparison among groups. The least significant difference test was used in the analysis of homogenous variance whereas Dunnett's T3 test was used in the analysis of heterogenous variance, and P value of < 0.05 was considered statistically significant.

3. RESULTS

3.1. Target prediction and ingredient analysis of QD

From the network pharmacology-based analysis using TCMSP, a total of 29 compounds had been identified in Qingdai (Indigo Naturalis) (a.k.a. QD). Among these identified compounds, 9 of them (Table 1) were selected as core active ingredients as they satisfied the screening criteria suggested by TCMSP (i.e. OB ≥ 30% and DL ≥ 0.18). A total of 58 putative targets of the core active compounds of QD had been retrieved *via* target fishing from various databases.

3.2. Identification of UC targets

By means of searching from relevant databases and utilizing text mining tools, 2104 UC-related targets had been attained. In consequence, we integrated the analytical results from different databases and combined with the GEO datasets to remove duplicates, 19

Table 1 Active compounds identified in QD

MOL_ID	molecule_name	OB (%)	DL
MOL000358	beta-sitosterol	36.91	0.75
MOL001781	Indigo	38.20	0.26
MOL001810	6-(3-oxoindolin-2-ylidene)indolo[2,1-b]quinazolin-12-one	45.28	0.89
MOL002309	indirubin	48.59	0.26
MOL002322	isovitexin	31.29	0.72
MOL011100	bisindigotin	41.66	0.39
MOL011105	indican	34.90	0.23
MOL011332	10h-indolo,[3,2-b],quinoline	54.57	0.22
MOL011335	Isoindigo	94.30	0.26

Notes: QD: Qingdai (*Indigo Naturalis*); OB: oral bioavailability; DL: drug-like properties.

overlapped targets (i.e. AHR, BCL2L1, CA2, ESR1, F2, GSK3B, IFNG, JUN, KDR, MAPK14, NOS2, NOS3, NR3C1, PDE3A, PON1, PPARG, PTGS1, PTGS2 and TNF) were eventually obtained (Figure 1A), which are the potential targets of the active ingredients of QD in the prevention and treatment of UC.

3.3. PPI network analysis

In order to illustrate the role of target proteins at the system level, the potential targets acquired in the previous sections were imported into STRING to eliminate the unconnected targets. By utilizing the Cytoscape 3.7.1 visualization software, the PPI network of QD was generated with 56 nodes and 272 edges (Figure 1B). The green nodes represent the targets of the core active ingredients of QD whereas the red nodes represent the composite targets of QD and UC. In the network, the higher the target degree, the larger the node size is. On the other hand, the PPI network of UC analysis was generated with 1423 nodes and 13335 edges (Figure 1C). The yellow nodes represent the potential targets of UC whereas red nodes represent the composite targets of QD and UC. By intersecting the PPI networks of QD and UC analysis, we constructed the network diagram of core targets of QD treatment against UC, which include 17 nodes and 77 edges (Figure 1D). The node size is proportional to the target degree of QD in the treatment of UC; these 17 targets were presented in a bar chart according to the degrees of the nodes (Figure 1E). The top 5 nodes were TNF, PTGS2, JUN, NOS3 and PPARγ. For a better visualization of the relationships among the TCM herb, its core active ingredients, the putative biological targets and disease, a TCM-active ingredients-targets-disease network diagram is provided in Figure 1F.

3.4. Enrichment analyses

GO analysis was performed to gain a further insight into the most plausible mechanisms of QD in the treatment of UC. To the 19 identified potential targets, with the false discovery rate (FDR) threshold set at < 0.05, a total of 1028 GO entries were identified (Figure 2A). These entries revealed that the protective mechanisms of QD are highly associated with a variety of biological processes, including small molecule metabolic process (GO:0044281), reactive oxygen species metabolic processes (GO:0072593), nitric oxide biosynthetic process (GO:0006809), reactive nitrogen species process (GO:2001057), as well as several molecular functions, such as nuclear receptor activity (GO:0004879), DNA-binding transcription factor activity (GO:0003700), RNA polymerase II Transcription factor binding (GO:0016251), Hsp90 protein binding (GO:0051879), etc… In addition, the KEGG enrichment analysis was also performed on the target of QD for the treatment of UC, and a total of 78 signal pathways were obtained. R language was used to plot the KEGG histogram (Figure 2B) whereas the degree of KEGG enrichment was determined by Rich factor, *P*-value and the number of genes enriched in the pathway. According to the highest numbers of genes, the highly associated pathways in the prevention and treatment of UC by QD include the IL-17 signaling pathway, T-cell receptor signaling pathway, VEGF signaling pathway as well as Th1 and Th2 cell differentiation.

3.5. QD decreased DAI scores and reduced colon shortening in DSS-induced colitis

In the 10-day experimental trial, the administration of DSS led to obvious clinical changes in the C57BL6 mice. After consuming 2% DSS water for 2 d, the hair color of the diseased mice became dull whilst their activities were notably reduced. Their stools were loose and the fecal occult blood test yielded a positive result. After 4 d of DSS induction, most of the mice in the DSS group curled up into a ball and showed other clinical signs of colitis, such as lean body mass (Figure 3A), withered hair, low body temperature and bloody stool. From day 5 onwards, black feces, or even fresh blood around the anus, were observed in all of the mice in the DSS group. On the contrary, the mice in the treatment groups (i.e. the 5-ASA+DSS group and QD + DSS group) increased food intake whereas their gross bloody stools diminished after 2 d of drug intervention; however, their result of fecal occult blood test was still positive. Seven days after drug intervention, many of them showed soft granular or ball-shaped stools, glossy hair and increased activity. At the end of the experiment, i.e. day 10 (Figure 3B), the DAI scores of the QD + DSS group (2.87 ± 0.23) and 5-ASA + DSS group (3.12 ± 0.23) were significantly lower than

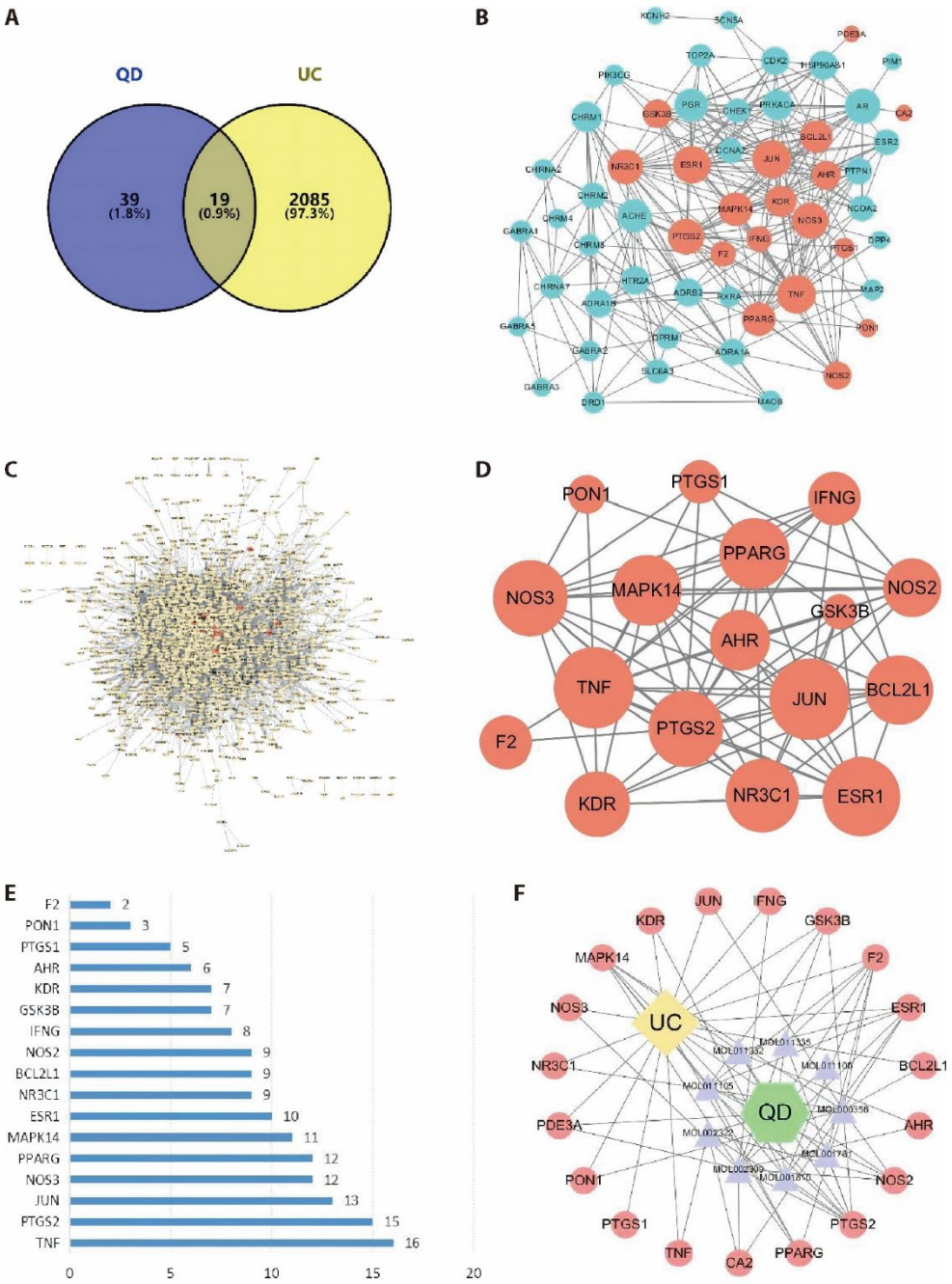

Figure 1 Results of network pharmacology-based analyses

A: after searching from a variety of databases, the Venn diagram summarizes the targets in UC and QD; B: by using the Cytoscape 3.7.1 visualization software, the PPI network of QD was generated with 56 nodes and 272 edges; C: the PPI network of UC analysis was generated with 1423 nodes and 13335 edges; D: the network diagram of core targets of QD treatment against UC, which include 17 nodes and 77 edges; E: 17 targets identified according to the degrees of the nodes presented in the previous figure; F: the ultimate TCM-active ingredients-targets-disease network diagram was generated upon the above analyses. BCL2L1: apoptosis regulator Bcl-2; CA2: carbonic anhydrase II; ESR1: estrogen receptor; F2: thrombin; GSK3B: glycogen synthase kinase-3 beta; JUN: transcription factor AP-1; MAPK14: mitogen-activated protein kinase 14; NOS2: nitric oxide synthase, inducible; NR3C1: glucocorticoid receptor; PDE3A: CGMP-inhibited 3',5'-cyclic phosphodiesterase A; PON1: serum paraoxonase/arylesterase 1; PPARG: peroxisome proliferator activated receptor gamma; PTGS2: prostaglandin G/H synthase 2; ESR1: estrogen receptor; KDR: vascular endothelial growth factor receptor 2; MAPK14: mitogen-activated protein kinase 14; AHR: aryl hydrocarbon receptor; CA2: carbonic anhydrase II; IFNG: interferon gamma; NOS3: nitric-oxide synthase, endothelial; TNF: tumor necrosis factor.

those of the DSS group (4.00 ± 0.16). Apart from the DAI scores, the severity of colitis was also implicated by the shortening of colon length. As shown in Figure 3C, the colons were shortened by more than 28% under colitis condition but were notably relieved by the treatment of QD.

3.6. QD restored mucosal architecture in DSS-induced colitis

The HE images revealed that the DSS induction notably disrupted the mucosal architecture of the colon, caused infiltration of lymphocytes and lymphoid follicles and increased the thickness of the muscle layer. Moreover,

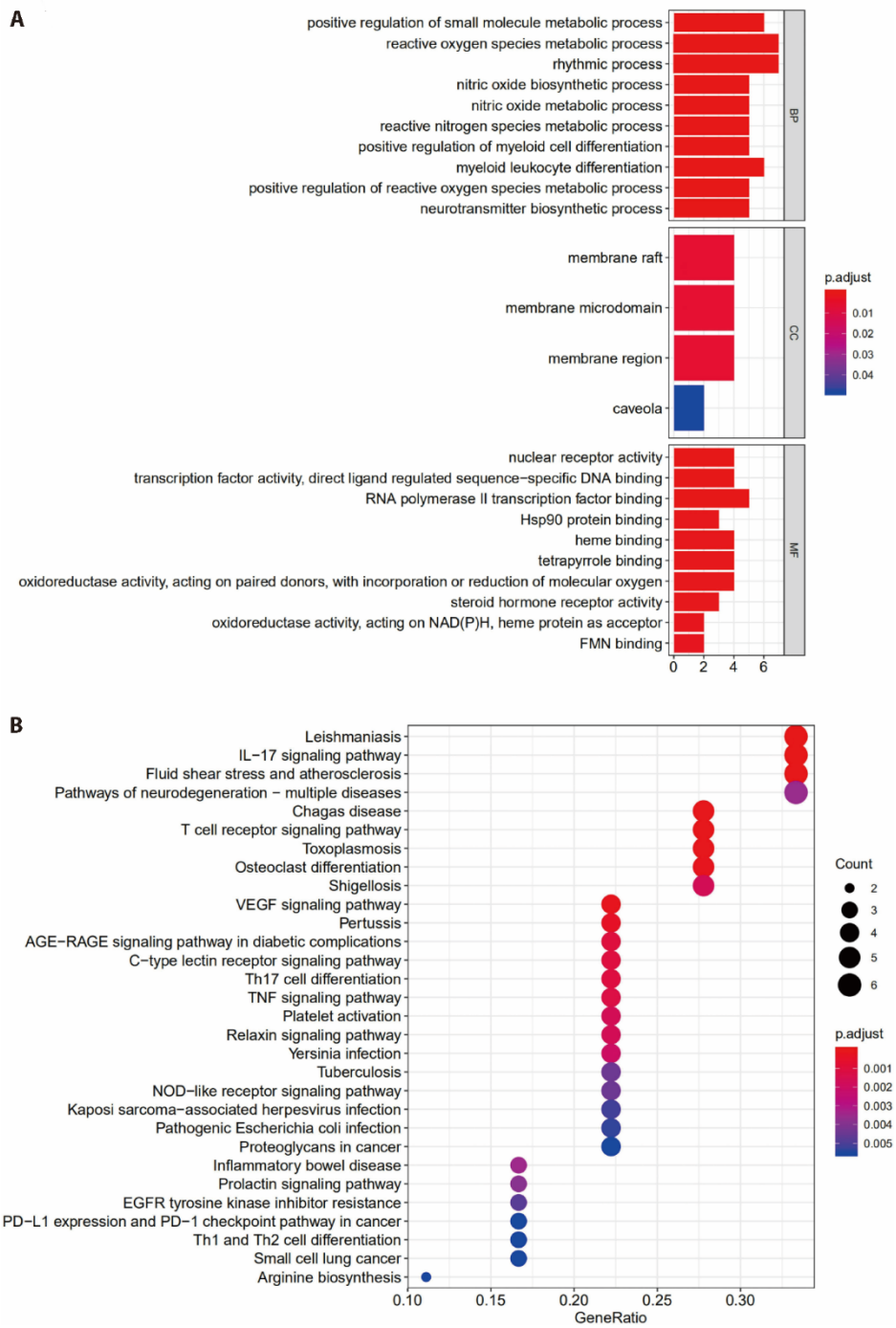

Figure 2 Results of enrichment analyses

A: a total of 1028 GO entries were identified from 19 potential targets upon the GO enrichment analysis; FDR < 0.05; B: a total of 78 signal pathways were obtained upon the KEGG enrichment analysis, R language was used to plot the KEGG histogram. GO: gene ontology; KEGG: Kyoto Encyclopedia of Genes and Genomes; FDR: false discovery rate; VEGF: vascular endothlial growth factor; PD-L1: programmed cell death-Ligand 1; TNF: tumor necrosis factor; NAD (P) H: dehydrogenase, quinone 2; FMN: flavinmononucleotide.

extensive necrosis, abscesses, ulcers, goblet cell death and irregular crypts were observed in the DSS-induced colonic tissues. In the QD + DSS group, the disruption of mucosal epithelia was significantly reduced whereas the number of intact crypts was considerably increased (Figure 4). Accompanied by the repair and hyperplasia of granulation tissue, tubular and thickened glands as well as the scattered lymphocytes and macrophages were retrieved in the lamina propria as shown in the zoom-in micrographs (Figure 4).

3.7. QD inhibited activation of the GSK3-β/FOXp3 axis in DSS-induced colitis

As GSK3-β and FOXP3 are important regulators of excessive inflammatory responses, we examined the effect of QD on these two pivotal factors in colitis. Our Western blotting results showed that the expression levels of GSK3-β and Foxp3 *in* colonic tissues of the DSS group were remarkably up-regulated when compared to those of the CON group. In addition, the

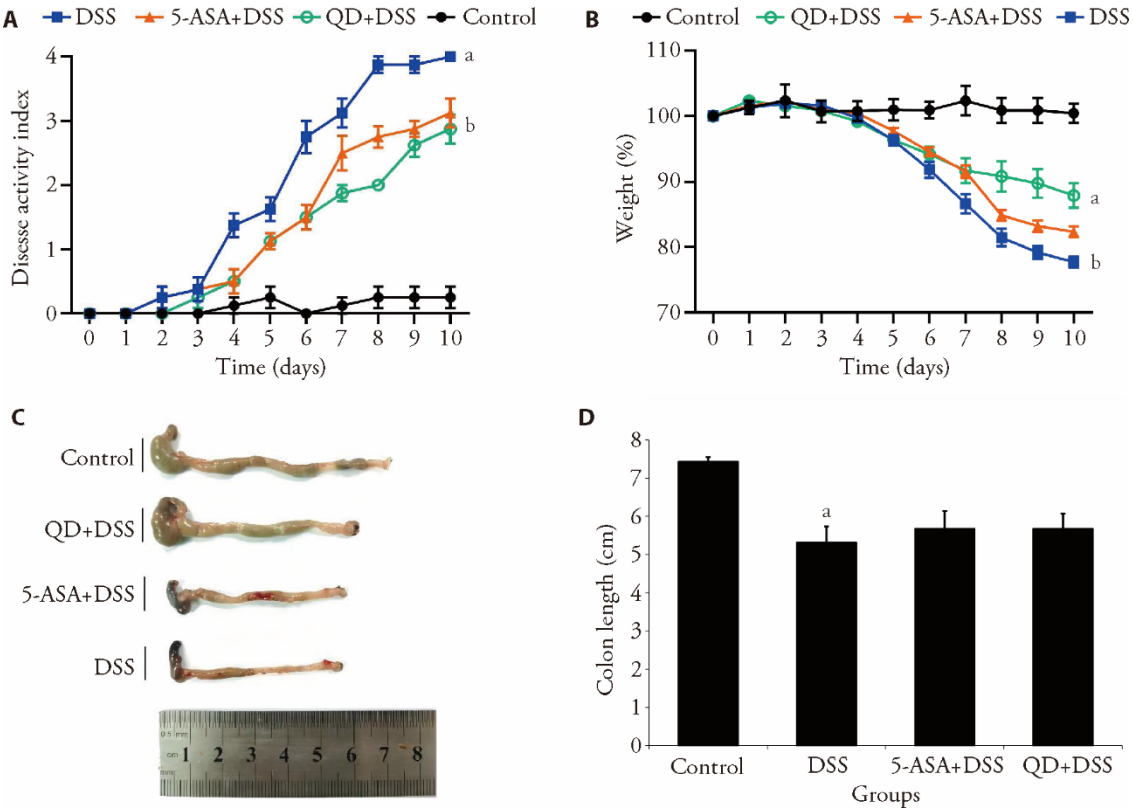

Figure 3 Ameliorative effect of QD on experimental colitis

A: change of body weight of each group was calculated as the percent difference between the original body weight at day 0 and the weight on any particular day during the experimental period. Values represent the averages of 8 mice; B: DAI scores of different experimental groups of mice; C: lengths of colons were measured at the time of sacrifice. Control group treating saline treatment control for 10 d. DSS group consuming 2.5% DSS water for 7 d followed by an additional consumption period of normal drinking water for 3 d. (5-ASA+DSS) group fed with 2.5% DSS, and respectively given with 5-ASA (o.g.; 100 mg·kg^{-1}·d^{-1}) from day 0 till the end of experiment for a total of 10 d. (QD+DSS) group fed with 2.5% DSS, and respectively given with QD (o.g.; 1.3 g raw herbs·kg^{-1}·d^{-1}) from day 0 till the end of experiment for a total of 10 d. QD: Qingdai (*Indigo Naturalis*); DAI: disease activity index; DSS: dextran sodium sulfate; 5-ASA: 5-aminosalicylic acid. $^{a}P < 0.005$, DSS group compared with Control groups; $^{b}P < 0.05$, (5-ASA+DSS) group compared with DSS groups.

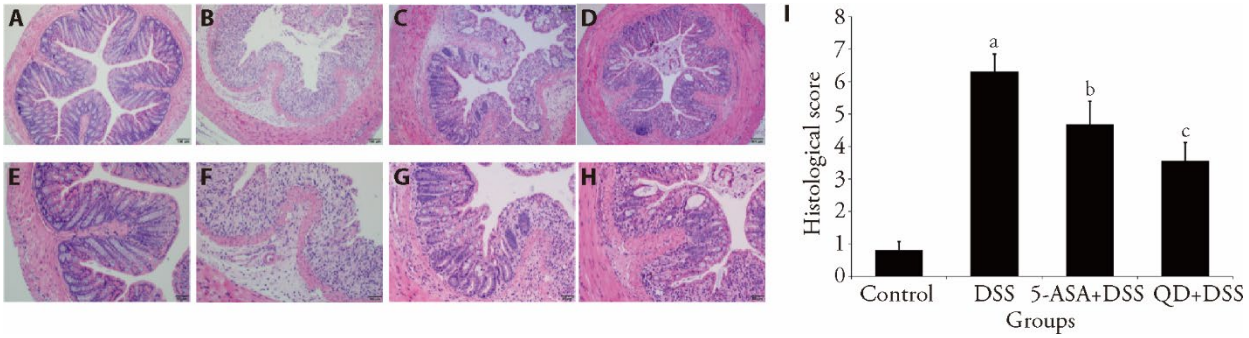

Figure 4 HE images revealing mucosal integrity in tissues in 10 d

A, H: mucosal integrity in tissues (× 100 and × 200) of control group treating saline treatment control for 10 d. B, E: mucosal integrity in tissues (×100 and ×200) of DSS group consuming 2.5% DSS water for 7 d followed by an additional consumption period of normal drinking water for 3 d. C, G: mucosal integrity in tissues (× 100 and × 200) of (5-ASA+DSS) group fed with 2.5% DSS, and respectively given with 5-ASA o.g.; 100 mg·kg^{-1}·d^{-1}) from day 0 till the end of experiment for a total of 10 d. D, H: mucosal integrity in tissues (× 100 and × 200) of (QD + DSS) group fed with 2.5% DSS, and respectively given with QD (o.g.; 1.3 g raw herbs·kg^{-1}·d^{-1}) from day 0 till the end of experiment for a total of 10 d. I: Histological scores were given based on the severity of colonic damages, lymphocyte infiltration and crypt disruption (n = 8/group). HE: hematoxylin-eosin; QD: Qingdai (*Indigo Naturalis*); DSS: dextran sodium sulfate; 5-ASA: 5-aminosalicylic acid. $^{a}P < 0.005$ DSS group compared with Control groups; $^{b}P < 0.05$, (5-ASA + DSS) group compared with DSS groups; $^{c}P < 0.05$, (QD + DSS) group compared with DSS groups.

phosphorylation of GSK3-β was also elevated in the inflamed colonic tissues (Figure S2, Table 2). When administered with QD, the activation of the GSK3-β/Foxp3 axis was signi-ficantly repressed in the diseased mice (Table 2). From our qRT-PCR results, we demonstrated that the 10-day intervention with QD notably suppressed the mRNA expression of GSK3-β in the colitic tissue whereas the transcript level of Foxp3 was retained (Table 2).

3.8. QD reduced pro-inflammatory mediators in DSS-induced colitis

It is well acknowledged that the production of pro-

inflammatory cytokines is positively correlated to the occurrence of tissue injury and development of inflammatory events. By means of ELISA, we observed that the colonic levels of TNF-α, IL-1β and IL-17A in the DSS-colitis mice were elevated by >70% when compared to those of the control animals. With the application of QD, the stimulated production of colonic TNF-α, IL-1β and IL-17a was largely suppressed (Table 4). Similar suppressive result was also observed in our qRT-PCR analysis as the mRNA level of TNF-α was significantly reduced in the colonic tissues of the QD + DSS group (Table 3).

4. DISCUSSION

Dysfunction of the intestinal mucosal immune system is critical to recurrent and prolonged UC, and an imbalance in T lymphocyte populations is a prerequisite for the dysfunction of mucosal immunity. According to the study by Sanchez-Munoz F and colleagues, the abnormal immune system of UC patients results from an imbalanced network of multifaceted cytokines and the sustained activation of immune cells.[22] GSK-3β signalling and Foxp3 activation are thought to be the key factors in the development and maintenance of regulatory T cell (Treg cell)-dependent inflammatory events.[23,24]

In recent years, Qingdai (*Indigo Naturalis, QD*) has been increasingly used in the treatment of various inflammatory diseases,[25] including ulcerative colitis. In fact, the unique features of TCM in the treatment of UC and related disorders are based on the restoration of *Qi* (or *Yin-Yang*) in the human body to achieve homeostasis. In terms of ancient TCM theories, the medicinal herb QD possesses several therapeutic properties, including detoxification, the clearance of "heat", nourishing the liver and blood cooling.[26,27] According to recent evidence-based studies, QD plays a hormone-like role in immunoregulation, as well as in some antibacterial and antitumour mechanisms.[28] Similar to Coptis chinensis,

Table 2 Expression levels of FOXP3, GSK-3β and p-GSK-3β in colonic by means of Western blotting ($\bar{x} \pm s$)

Group	*n*	FOXP3	GSK-3β	p-GSK-3β
Control	8	0.10±0.04	0.05±0.14	0.10±0.04
DSS	8	0.55±0.95[a]	0.38±0.08	0.55±0.95[a]
5-ASA+DSSS	8	1.46±0.18[b]	0.15±0.61[b]	0.27±0.08[b]
QD+DSS	8	1.37±0.18[c]	0.13±0.50[c]	0.31±0.08[c]

Notes: control: treated only phydiological saline for 10 d; DSS: consuming 2.5% DSS water for 7 d followed by an additional consumption period of normal drinking water for 3 d; 5-ASA + DSS: fed with 2.5% DSS, and respectively given with 5-ASA (o.g.; 100 $mg \cdot kg^{-1} \cdot d^{-1}$) from day 0 till the end of experiment for a total of 10d. QD + DSS: fed with 2.5% DSS, and respectively given with QD (o.g.; 1.3 g raw herbs$\cdot kg^{-1} \cdot d^{-1}$) from day 0 till the end of experiment for a total of 10 d. FOXP3: forkhead box protein 3; GSK-3β: glycogen synthase kinase-3 beta; p-GSK-3β: phospho-glycogen synthase kinase-3 beta; DSS: dextran sodium sulfate; 5-ASA: 5-aminosalicylic acid; QD: Qingdai (*Indigo Naturalis*). [a]$P < 0.005$ DSS group compared with Control groups; [b]$P < 0.05$, (5-ASA + DSS) group compared with DSS groups; [c]$P < 0.01$, (QD + DSS) group compared with DSS groups.

Table 3 qRT-PCR results showed the regulation of mRNA levels of GSK-3β, TNF-α and FOXP3 in the colonic tissues of experimental mice (%, $\bar{x} \pm s$)

Group	*n*	GSK-3β	TNF-α	FOXP3
Control	8	1.00±0.07	1.03±0.13	1.04±0.13
DSS	8	2.15±0.22[a]	4.29±0.60[a]	0.43±0.06[a]
5-ASA+DSS	8	1.46±0.18[b]	2.65±0.73[b]	0.82±0.06[b]
QD+DSS	8	1.37±0.18[c]	2.20±0.51[c]	0.70±0.16[c]

Notes: control: treated only phydiological saline for 10 d; DSS: consuming 2.5% DSS water for 7 d followed by an additional consumption period of normal drinking water for 3 d; 5-ASA + DSS: fed with 2.5% DSS, and respectively given with 5-ASA (o.g.; 100 $mg \cdot kg^{-1} \cdot d^{-1}$) from day 0 till the end of experiment for a total of 10 d. QD + DSS: fed with 2.5% DSS, and respectively given with QD (o.g.; 1.3 g raw herbs$\cdot kg^{-1} \cdot d^{-1}$) from day 0 till the end of experiment for a total of 10 d. qRT-PCR: real-time quantitative polymerase chain reaction; FOXP3: forkhead box protein 3; GSK-3β: glycogen synthase kinase-3 beta; TNF-α: tumor necrosis factor -α; DSS: dextran sodium sulfate; 5-ASA: 5-aminosalicylic acid; QD: Qingdai (*Indigo Naturalis*). [a]$P < 0.005$ DSS group compared with Control groups; [b]$P < 0.05$, (5-ASA + DSS) group compared with DSS groups; [c]$P < 0.01$, (QD + DSS) group compared with DSS groups.

Table 4 Colonic levels of pro-inflammatory cytokines TNF-α, IL-1β and IL-17A were evaluated using ELISAs (pg/mL mg per tissue, $\bar{x} \pm s$)

Group	*n*	IL-1β	TNF-α	IL-17A
Control	8	4.15±0.84	14.30±1.2	2.63±0.78
DSS	8	19.11±1.75[a]	97.25±9.68[a]	8.59±2.41[a]
5-ASA+DSS	8	10.93±0.99[b]	37.83±8.41[b]	3.83±0.98[b]
QD+DSS	8	11.20±0.55[c]	47.24±6.05[c]	3.24±1.32[c]

Notes: control: treated only phydiological saline for 10 d; DSS: consuming 2.5% DSS water for 7 d followed by an additional consumption period of normal drinking water for 3 d; 5-ASA + DSS: fed with 2.5% DSS, and respectively given with 5-ASA (o.g.; 100 $mg \cdot kg^{-1} \cdot d^{-1}$) from day 0 till the end of experiment for a total of 10 d. QD + DSS: fed with 2.5% DSS, and respectively given with QD (o.g.; 1.3 g raw herbs$\cdot kg^{-1} \cdot d^{-1}$) from day 0 till the end of experiment for a total of 10 d. ELISA: enzyme-linked immunosorbent assay; DSS: dextran sodium sulfate; 5-ASA: 5-aminosalicylic acid; QD: Qingdai (*Indigo Naturalis*); IL-1β: interleukin 1β; TNF-α: tumor necrosis factor -α; IL-17A: Interleukin 17A. [a]$P < 0.005$, DSS group compared with Control groups; [b]$P < 0.05$, (5-ASA + DSS) group compared with DSS groups; [c]$P < 0.01$, (QD + DSS) group compared with DSS groups.

another common anti-inflammatory herb, the detoxification and heat clearing effects of QD are highly associated with the inhibition of GSK-3β signalling.[27] Therefore, both QD and C. chinensis are considered effective GSK-3β inhibitors, as they have been demonstrated to suppress GSK-3β-mediated cellular differentiation, migration and apoptosis.[26] In mouse models of colitis induced by DSS or TNBS, the use of GSK-3β inhibitors was effective in reducing the severity of inflammation and tissue injury in the colon.[29,30] However, the protective mechanisms remained unclear. In this study, we also observed that 10 d of oral QD administration led to decreased expression of GSK-3β and suppressed GSK-3β phosphorylation in the colonic tissues of diseased mice, and the DAI scores were notably decreased.

GSK-3 is a member of the serine/threonine kinase family and exists as two subtypes, GSK-3α and GSK-3β, which are the key kinases in glucose metabolism.[31] A growing body of evidence suggests that GSK-3 also plays important roles in biological processes in the human body, including protein synthesis, cell proliferation and differentiation and the immune response, in addition to carbohydrate metabolism.[32,33] In the regulation of inflammatory diseases, namely, arthritis and multiple sclerosis, GSK-3 signalling is critical in the activation of the pivotal transcription factor nuclear factor kappa B (NF-κB) and the subsequent release of proinflammatory mediators, including TNF-α, IL-1β and IL-6.[34,35] Furthermore, the GSK-3β signaling pathway was demonstrated to play a very important role in the modulation of Th17 cell differentiation and the immunosuppressive activity of Treg cells.[36] Beurel et al. showed that the protein level of GSK-3β was elevated by nearly 10 times in differentiated Th17 cells.[31] In contrast, the inhibition of GSK-3β signaling led to a significant decrease in IL-6 production and STAT3-dependent Th17 differentiation. In mice with encephalomyelitis, the use of GSK-3β inhibitors effectively suppressed the number of CD4+ Th17 cells, which are the major source of IL-17A.[37] Undoubtedly, IL-17 is a versatile cytokine involved in host defence and tissue repair. In our current work, the use of QD significantly reduced the colonic level of IL-17A in DSS mice and consequently resulted in the alleviation of colitis.

According to a study by Graham *et al*,[37] FOXP3 expression was considerably stabilized in Treg cells after the administration of GSK-3β inhibitors, and the expression levels of β-catenin and the antiapoptotic protein Bcl-xl in Treg cells were accordingly enhanced. In fact, FOXP3 is mainly expressed in secondary lymphoid organs, such as the spleen and lymph nodes, and plays an essential role in the development of Treg cells.[23] As a result, regulation of the GSK-3β/FOXP3 axis appears to be extremely crucial in the development of prolonged inflammatory events and apoptotic cell death.

In the current study, we demonstrated that oral administration of QD for 10 d significantly protected DSS-induced mice from severe colitis. The underlying protective mechanism involved not only the suppression of GSK-3β signalling but also the stabilization of Foxp3 mRNA levels in colitis tissues. In addition to the reduced production of proinflammatory cytokines by GSK-3β inhibition, FOXP3 stabilization in Treg cells is also crucial for antiapoptotic events and the amelioration of epithelial damage. In clinical cases, the levels of Th17/Treg-dependent cytokines, namely, IL-1β, IL-6 and IL-23, were significantly elevated in patients with immune diseases.[38,39] It is widely acknowledged that an imbalance in Th17 cells, Treg cells and their corresponding cytokines results in the breakage of autoimmune tolerance and consequently leads to tissue damage and inflammatory events.[40] Taken together, we believe that the effect of GSK-3β inhibition by the core active components of QD was derived from its regulation of Th17 cells and Treg cells.

With the aid of network pharmacology-based analysis, we were able to predict the core active components of QD that contribute the most ameliorating effects in the treatment of UC. To further elucidate the protective mechanisms of QD, we used LC/MS to quantify the individual active components of QD and performed corresponding pharmacokinetic and metabonomic analysis of each of them. In addition, we may need to use cellular and animal models to validate the relevant signaling pathways and biological targets of the active ingredients of QD.

In conclusion, the results of this study provide solid scientific evidence for the use of QD or its core active components in the clinical management of UC.

5. REFERENCES

1. Ungaro R, Mehandru S, Allen PB, Peyrin-Biroulet L, Colombel JF. Ulcerative colitis. Lancet 2017; 389: 1756-70.
2. Doherty G, Katsanos KH, Burisch J, et al. European crohn's and colitis organisation topical review on treatment withdrawal ['exit strategies'] in inflammatory bowel disease. J Crohns Colitis 2018; 12: 17-31.
3. Zhao L, Zhang S, He P. Mechanistic understanding of herbal therapy in inflammatory bowel disease. Curr Pharm Des 2017; 23: 5173-79.
4. Yang Y, Zhang Z, Li S, Ye X, Li X, He K. Synergy effects of herb extracts: pharmacokinetics and pharmacodynamic basis. Fitoterapia 2014; 92: 133-47.
5. Shimada F, Yoshimatsu Y, Sujino T, Fukuda T, Naganuma M, Kanai T. Su473 natural history after the induction therapy in uc patients with indigo naturalis. Gastroenterology 2021; 160: S-708.
6. Antonio-Cisneros CM, Dávila-Jiménez MM, Elizalde-González MP, García-Díaz E. Tio2 immobilized on manihot carbon: Optimal preparation and evaluation of its activity in the decomposition of indigo carmine. Int J Mol Sci 2015; 16: 1590-612.
7. Li S. Framework and practice of network-based studies for Chinese herbal formula. Zhong Xi Yi Jie He Xue Bao 2007; 5: 489-93.
8. Ru J, Li P, Wang J, et al. TCMSP: a database of systems pharmacology for drug discovery from herbal medicines. J Cheminform 2014; 6: 13.
9. Liu Z, Guo F, Wang Y, et al. Batman-TCM: a bioinformatics analysis tool for molecular mechanism of Traditional Chinese Medicine. Sci Rep 2016; 6: 21146.

10. Xue R, Fang Z, Zhang M, Yi Z, Wen C, Shi T. TCMID: Traditional Chinese Medicine integrative database for herb molecular mechanism analysis. Nucleic Acids Res 2013; 41: D1089-95.
11. Daina A, Michielin O, Zoete V. Swisstargetprediction: updated data and new features for efficient prediction of protein targets of small molecules. Nucleic Acids Res 2019; 47: W357-64.
12. Liu X, Ouyang S, Yu B, et al. Pharmmapper server: a web server for potential drug target identification using pharmacophore mapping approach. Nucleic Acids Res 2010; 38: W609-14.
13. Shannon P, Markiel A, Ozier O, et al. Cytoscape: a software environment for integrated models of biomolecular interaction networks. Genome Res 2003; 13: 2498-504.
14. Hamosh A, Scott AF, Amberger J, Bocchini C, Valle D, McKusick VA. Online mendelian inheritance in man (omim), a knowledgebase of human genes and genetic disorders. Nucleic Acids Res 2002; 30: 52-5.
15. Yang H, Qin C, Li YH, et al. Therapeutic target database update 2016: enriched resource for bench to clinical drug target and targeted pathway information. Nucleic Acids Res 2016; 44: D1069-74.
16. Thorn CF, Klein TE, Altman RB. Pharmgkb: the pharmacogenomics knowledge base. Methods Mol Biol 2013; 1015: 311-20.
17. Kim J, So S, Lee HJ, Park JC, Kim JJ, Lee H. Digsee: disease gene search engine with evidence sentences (version cancer). Nucleic Acids Res 2013; 41: W510-7.
18. Mandloi S, Chakrabarti S. Palm-ist: pathway assembly from literature mining--an information search tool. Sci Rep 2015; 5: 10021.
19. Liu Y, Liang Y, Wishart D. Polysearch2: a significantly improved text-mining system for discovering associations between human diseases, genes, drugs, metabolites, toxins and more. Nucleic Acids Res 2015; 43: W535-42.
20. de Leeuw N, Dijkhuizen T, Hehir-Kwa JY, et al. Diagnostic interpretation of array data using public databases and internet sources. Hum Mutat 2012; 33: 930-40.
21. Szklarczyk D, Morris JH, Cook H, et al. The string database in 2017: quality-controlled protein-protein association networks, made broadly accessible. Nucleic Acids Res 2017; 45: D362-8.
22. Sanchez-Munoz F, Dominguez-Lopez A, Yamamoto-Furusho JK. Role of cytokines in inflammatory bowel disease. World J Gastroenterol 2008; 14: 4280-8.
23. Schubert LA, Jeffery E, Zhang Y, Ramsdell F, Ziegler SF. Scurfin (foxp3) acts as a repressor of transcription and regulates t cell activation. J Biol Chem 2001; 276: 37672-9.
24. Fontenot JD, Gavin MA, Rudensky AY. Foxp3 programs the development and function of CD4+CD25+ regulatory t cells. Nat Immunol 2003; 4: 330-6.
25. Naganuma M. Treatment with indigo naturalis for inflammatory bowel disease and other immune diseases. Immunol Med 2019; 42: 16-21.
26. Leclerc S, Garnier M, Hoessel R, et al. Indirubins inhibit glycogen synthase kinase-3 beta and cdk5/p25, two protein kinases involved in abnormal tau phosphorylation in alzheimer's disease. A property common to most cyclin-dependent kinase inhibitors? J Biol Chem 2001; 276: 251-60.
27. Eisenbrand G, Hippe F, Jakobs S, Muehlbeyer S. Molecular mechanisms of indirubin and its derivatives: Novel anticancer molecules with their origin in traditional Chinese phytomedicine. J Cancer Res Clin Oncol 2004; 130: 627-35.
28. Xiao HT, Peng J, Wen B, et al. Indigo naturalis suppresses colonic oxidative stress and th1/th17 responses of dss-induced colitis in mice. Oxid Med Cell Longev 2019; 2019: 9480945.
29. Hofmann C, Dunger N, Schölmerich J, Falk W, Obermeier F. Glycogen synthase kinase 3-β: a master regulator of toll-like receptor-mediated chronic intestinal inflammation. Inflamm Bowel Dis 2010; 16: 1850-8.
30. Whittle BJ, Varga C, Pósa A, Molnár A, Collin M, Thiemermann C. Reduction of experimental colitis in the rat by inhibitors of glycogen synthase kinase-3beta. Br J Pharmacol 2006; 147: 575-82.
31. Beurel E, Grieco SF, Jope RS. Glycogen synthase kinase-3 (gsk3): regulation, actions, and diseases. Pharmacol Ther 2015; 148: 114-31.
32. Elson CO, Cong Y, Weaver CT, et al. Monoclonal anti-interleukin 23 reverses active colitis in a t cell-mediated model in mice. Gastroenterology 2007; 132: 2359-70.
33. Takahashi-Yanaga F. Activator or inhibitor? Gsk-3 as a new drug target. Biochem Pharmacol 2013; 86: 191-9.
34. Cortés-Vieyra R, Bravo-Patiño A, Valdez-Alarcón JJ, Juárez MC, Finlay BB, Baizabal-Aguirre VM. Role of glycogen synthase kinase-3 beta in the inflammatory response caused by bacterial pathogens. J Inflamm (Lond) 2012; 9: 23.
35. Mi H, Liu FB, Li HW, Hou JT, Li PW. Anti-inflammatory effect of chang-an-shuan on tnbs-induced experimental colitis in rats. BMC Complement Altern Med 2017; 17: 315.
36. Harada K, Shimoda S, Sato Y, Isse K, Ikeda H, Nakanuma Y. Periductal interleukin-17 production in association with biliary innate immunity contributes to the pathogenesis of cholangiopathy in primary biliary cirrhosis. Clin Exp Immunol 2009; 157: 261-70.
37. Graham JA, Fray M, de Haseth S, et al. Suppressive regulatory t cell activity is potentiated by glycogen synthase kinase 3{beta} inhibition. J Biol Chem 2010; 285: 32852-59.
38. Cosmi L, Santarlasci V, Maggi L, Liotta F, Annunziato F. Th17 plasticity: pathophysiology and treatment of chronic inflammatory disorders. Curr Opin Pharmacol 2014; 17: 12-6.
39. Romagnani S, Maggi E, Liotta F, Cosmi L, Annunziato F. Properties and origin of human th17 cells. Mol Immunol 2009; 47: 3-7.
40. Annunziato F, Cosmi L, Liotta F, Maggi E, Romagnani S. The phenotype of human th17 cells and their precursors, the cytokines that mediate their differentiation and the role of th17 cells in inflammation. Int Immunol 2008; 20: 1361-8.